

LETTERS

Chemical characterization of element 112

R. Eichler^{1,2}, N. V. Aksenov³, A. V. Belozerov³, G. A. Bozhikov³, V. I. Chepigin³, S. N. Dmitriev³, R. Dressler¹, H. W. Gäggeler^{1,2}, V. A. Gorshkov³, F. Haenssler^{1,2}, M. G. Itkis³, A. Laube¹, V. Ya. Lebedev³, O. N. Malyshev³, Yu. Ts. Oganessian³, O. V. Petrushkin³, D. Piguet¹, P. Rasmussen¹, S. V. Shishkin³, A. V. Shutov³, A. I. Svirikhin³, E. E. Tereshatov³, G. K. Vostokin³, M. Wegrzecki⁴ & A. V. Yeremin³

The heaviest elements to have been chemically characterized are seaborgium¹ (element 106), bohrium² (element 107) and hassium³ (element 108). All three behave according to their respective positions in groups 6, 7 and 8 of the periodic table, which arranges elements according to their outermost electrons and hence their chemical properties. However, the chemical characterization results are not trivial: relativistic effects on the electronic structure of the heaviest elements can strongly influence chemical properties^{4–6}. The next heavy element targeted for chemical characterization is element 112; its closed-shell electronic structure with a filled outer *s* orbital suggests that it may be particularly susceptible to strong deviations from the chemical property trends expected within group 12. Indeed, first experiments concluded that element 112 does not behave like its lighter homologue mercury^{7–9}. However, the production and identification methods^{10,11} used cast doubt on the validity of this result. Here we report a more reliable chemical characterization of element 112, involving the production of two atoms of ²⁸³112 through the alpha decay of the short-lived ²⁸⁷114 (which itself forms in the nuclear fusion reaction¹² of ⁴⁸Ca with ²⁴²Pu) and the adsorption of the two atoms on a gold surface. By directly comparing the adsorption characteristics of ²⁸³112 to that of mercury and the noble gas radon, we find that element 112 is very volatile and, unlike radon, reveals a metallic interaction with the gold surface. These adsorption characteristics establish element 112 as a typical element of group 12, and its successful production unambiguously establishes the approach to the island of stability of superheavy elements through ⁴⁸Ca-induced nuclear fusion reactions with actinides.

Element 112 was discovered¹³ at the Gesellschaft für Schwerionenforschung (GSI), Darmstadt, Germany in 1996. It was produced as an isotope with mass number 277 in the nuclear fusion reaction of ⁷⁰Zn with ²⁰⁸Pb, but its measured half-life of about 200 μ s was too short for a chemical investigation. Three years later, the Flerov Laboratory for Nuclear Reactions (FLNR), Dubna, Russia, announced¹⁴ the production of elements 112 and 114 in nuclear fusion reactions of ⁴⁸Ca with ²³⁸U and ²⁴²Pu. For isotope ²⁸³112, the study indicated¹⁴ a half-life of about 3 min and decay through pure spontaneous fission, confirmed in a later experiment¹⁵. The first studies to chemically characterize this isotope were conducted at FLNR and GSI and suggested^{7–9} that element 112 does not behave like mercury, its lighter homologue in group 12 of the periodic table. However, the identification of element 112 in these studies was uncertain because it relied only on the observation of unspecific spontaneous-fission decay events. A new series of physics experiments at the FLNR in 2004 revealed¹² other decay properties for ²⁸³112: decay through emission of a 9.5-MeV alpha particle and a half-life of about

4 s, followed by the spontaneous fission decay of ²⁷⁹110 with a half-life of about 0.2 s. Moreover, physics experiments at the Lawrence Berkeley National Laboratory, Berkeley, USA¹⁰, and chemistry experiments performed at GSI¹¹ failed to observe element 112 in the nuclear fusion reaction of ⁴⁸Ca with ²³⁸U, which was used in the earlier investigations. In view of these difficulties, for this experiment we used the nuclear fusion of ⁴⁸Ca and ²⁴²Pu, in which ²⁸³112 was reported¹² to be produced as the alpha decay daughter of the primary reaction product ²⁸⁷114 at a rate of several atoms per week.

The systematic order of the periodic table places element 112 in group 12, which also includes zinc, cadmium and mercury. It should thus have the closed-shell electronic ground state configuration Rn: $5f^{14}6d^{10}7s^2$, which implies noble metal characteristics¹⁶. However, relativistic calculations of atomic properties of superheavy elements suggest^{4–6} contraction of the spherical *s*- and *p*_{1/2}-electron orbitals. The effect may increase the chemical stability of the elemental atomic state of element 112 beyond that of a noble metal and endow it with inertness more similar to that of the noble gas radon¹⁷, although recent relativistic calculations on element 112 predicted¹⁸ that it should form a semiconductor-like solid with clear chemical bonds. It was suggested¹⁹ that the questions of the bonding characteristics of element 112 and whether it more strongly resembles a noble metal or a noble gas might be addressed experimentally, by determining its gas adsorption properties on a noble metal surface such as gold.

In fact, relativistic calculations indicate that the spin-orbit splitting of the *6d* orbitals results in element 112 having a ground-state configuration with a *6d*_{5/2} outermost valence orbital, which would make it behave like a noble transition metal^{20,21}. Moreover, relativistic density functional calculations of its interaction with noble metals predict metallic interactions similar to those of the lighter homologue mercury^{22–24}. In the case of large gold clusters and one atom of element 112, the calculations indicate an interaction energy of $-\Delta H_{\text{ads}}^{\text{Au}}(\text{E112}) = 80 \pm 20 \text{ kJ mol}^{-1}$ (refs 23, 24). This result compares well with an adsorption enthalpy estimate from a semi-empirical macroscopic metal–metal adsorption model^{19,25,26}, which yields $-\Delta H_{\text{ads}}^{\text{Au}}(\text{E112}) = 83 \text{ kJ mol}^{-1}$ for a metal-like element 112 on gold^{25,26}; in contrast, the adsorption enthalpy for a noble-gas-like element 112 on gold surfaces was estimated to be $-\Delta H_{\text{ads}}^{\text{Au}}(\text{E112}) = 30 \pm 5 \text{ kJ mol}^{-1}$ (ref. 27). The range of values predicted for the two extreme cases needs to be taken into account when designing the experiment, to ensure that element 112 is detected irrespective of whether it exhibits the adsorption properties of a noble metal or a noble gas.

Thermochromatography allows very efficient probing of the interaction potential of volatile gas-phase species with stationary surfaces over a broad range of interaction enthalpies. We used the *in situ* volatilization and on-line detection method²⁸ for thermochromatography

¹Paul Scherrer Institute, 5232 Villigen, Switzerland. ²Department of Chemistry and Biochemistry, University of Bern, 3012 Bern, Switzerland. ³Flerov Laboratory of Nuclear Reactions, Joint Institute for Nuclear Research, 141980 Dubna, Russia. ⁴Institute of Electron Technology, 02-668 Warsaw, Poland.

measurements at temperatures between $+35\text{ }^{\circ}\text{C}$ and $-186\text{ }^{\circ}\text{C}$, with the original system modified and significantly improved^{11,29} to enable gas adsorption investigations of element 112 on gold surfaces. Figure 1 depicts schematically the experimental set-up. A target of $^{242}\text{PuO}_2$ (1.4 mg cm^{-2} ^{242}Pu) with an admixture of $^{\text{nat}}\text{Nd}_2\text{O}_3$ ($15\text{ }\mu\text{g cm}^{-2}$ of Nd of natural isotopic composition) was deposited on a thin (0.7 mg cm^{-2}) Ti backing foil and irradiated for about three weeks at the U-400 cyclotron at FLNR with 3.1×10^{18} ^{48}Ca particles at a primary energy of $270 \pm 3\text{ MeV}$. The beam energy in the middle of the target was $236 \pm 3\text{ MeV}$, corresponding to the maximum of the production cross-section of $^{287}\text{114}$ in the $^{242}\text{Pu}(^{48}\text{Ca}, 3n)$ reaction channel¹². The irradiation generated not only $^{287}\text{114}$, but also the partially alpha-decaying nuclide ^{185}Hg with a half-life of 49 s. This nuclide is produced in the reaction $^{142}\text{Nd}(^{48}\text{Ca}, 5n)$ and serves in our experiment as a monitor for the production and separation process. Various isotopes of radon (for example, ^{219}Rn , with a half-life of 4 s) were also produced in multi-nucleon transfer reactions between ^{48}Ca and ^{242}Pu . Thus, radon and mercury were studied simultaneously with element 112 throughout the experiment.

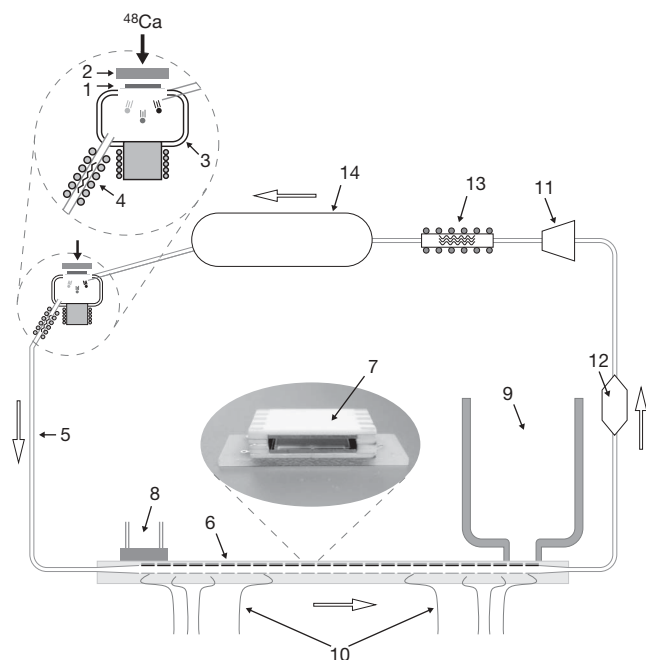


Figure 1 | Schematic experimental set-up used to investigate the adsorption properties of element 112 on a gold surface. A ^{242}Pu target of thickness 1.4 mg cm^{-2} (1) is irradiated by a ^{48}Ca beam that passes through a $4\text{-}\mu\text{m}$ Ti vacuum window (2). The reaction products recoil out of the target through the Ti target backing of $1.5\text{ }\mu\text{m}$ thickness into a recoil stopping volume of 35 cm^3 (3) that is flushed with a 850 ml min^{-1} He/Ar mixture (70/30 vol.%). This carrier gas transported the volatile nuclear reaction products through a quartz wool filter heated to $850\text{ }^{\circ}\text{C}$ (4) and a 8-m-long perfluoroalkoxy-Teflon capillary (5) to the thermochromatographic COLD detector array (6), which consists of 32 pairs of ion-implanted planar silicon detectors facing each other and forming a narrow chromatographic channel (7). One side of the channel is covered with a 50-nm-thick gold layer, deposited directly on the silicon detector surface. A temperature gradient was established along the detector array using a thermostat (8) at the entrance and a liquid nitrogen cryostat (9) at the exit and permanently monitored by eight PT100 platinum resistance thermometers (10) installed along the COLD detector. A self-drying closed gas loop system was developed to keep the amount of trace gases such as oxygen and water in this carrier gas mixture as low as possible. For this purpose the gas flow, enforced by a metal bellows pump (11), is permanently dried by passing it through a drying unit (12) containing Sicapent (a mixture of silica zeolites and phosphorus pentaoxide) and through a getter oven (13) containing tantalum and heated to $1000\text{ }^{\circ}\text{C}$. The gas pulsations originating from the pump are absorbed by a 10-litre buffer volume (14). The white arrows indicate the direction of the gas flow.

The nuclear reaction products passed the backing foil and were stopped in the recoil chamber flushed by the carrier gas. The chamber was covered inside by a quartz inlay (except for the copper beam stop) to avoid losses of element 112 due to adsorption on metallic surfaces. Aerosol particles produced by beam-induced sputtering processes on the copper were stopped directly behind the outlet of the recoil chamber on a quartz wool filter, kept in an oven at $850\text{ }^{\circ}\text{C}$. Additionally, a tantalum foil was inserted into this oven to chemically trap any traces of water and oxygen present in the carrier gas. This set-up guaranteed that only volatile nuclear reaction products entered the perfluoroalkoxy-Teflon capillary (length 8 m , inner diameter 1.56 mm) leading to the detection system. An average transport time from the production place to the detector of about 3.6 s was measured using ^{185}Hg .

The cryo-on-line detector (COLD) consists of an array of 32 pairs of ion-implanted planar silicon detectors ($9.7 \times 9.7\text{ mm}^2$ active area), with the active surfaces facing each other to form a rectangular channel with an open cross-section of $11.6 \times 1.5\text{ mm}^2$. The surface of the detectors on one side of the channel was covered by a $30\text{--}50\text{-nm}$ gold layer, while the other side retained the original silicon detector quartz surface that is chemically inert for the elemental state of most elements. The temperature gradient was established along this chromatographic channel by a thermostat heating at the inlet and a liquid-nitrogen cryostat cooling near the outlet. The event-by-event measurement of alpha and spontaneous fission decays provided an on-line identification of nuclides that were deposited on the gold surface in detection geometry close to 4π . Only decays related to the transported volatile nuclides ^{185}Hg , $^{219\text{--}221}\text{Rn}$, and $^{209\text{--}211}\text{At}$ were observed in the acquired alpha spectra. Mainly owing to the presence of the carrier gas in the detector array the spectroscopic resolution was about 120 keV . The overall transport and separation efficiencies were 90% and 56% for ^{185}Hg ($T_{1/2} = 49\text{ s}$) and ^{219}Rn ($T_{1/2} = 4\text{ s}$), respectively. The detection efficiencies for alpha decay of a species deposited on the detector surface was 87% . Accordingly, the efficiency of detecting an alpha-spontaneous fission (one fragment) or an alpha-spontaneous fission (two coincident fragments) was 87% or 75% , respectively.

During the experiment, two genetically linked decay chains were detected (Fig. 2). They were the only instances for which spontaneous

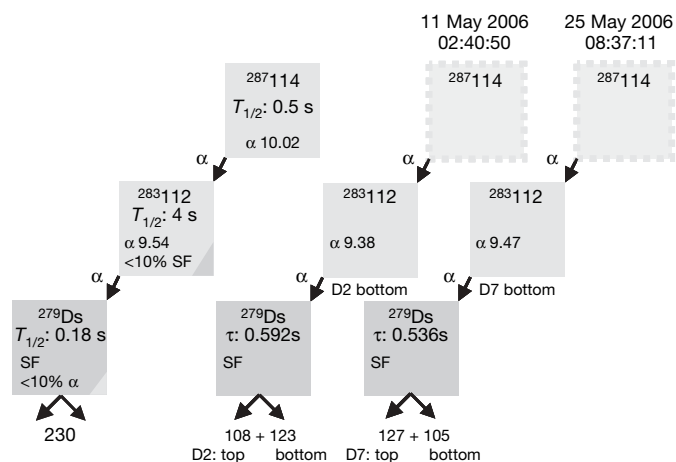


Figure 2 | The observed decay properties of $^{283}\text{112}$ and ^{279}Ds . The two decay chains observed in the COLD thermochromatography detector and attributed to the decay of $^{283}\text{112}$ are shown on the right side in comparison to the reported decay properties of $^{283}\text{112}$ on the left side¹². These decay chains allowed for the unambiguous identification of element 112 after the chemical separation. The alpha- and spontaneous-fission (SF) decay energies are given in MeV. The alpha spectroscopic resolution was about 0.12 MeV . The spontaneous-fission fragment energy resolution is about 20 MeV . The detector (D) number and the distribution of the decay chains in the detector pairs (top or bottom) are indicated. The top detector is gold covered.

fission fragments were measured throughout the entire experiment. The coincident detection of both spontaneous fission fragments revealed a total kinetic energy of about 230 MeV, which is typical for the spontaneous fission decay of a very heavy nucleus¹². Moreover, the observed spontaneous fission events were accompanied by detection of single high-energy alpha decays (9.38 ± 0.12 MeV and 9.47 ± 0.12 MeV, respectively) in the same detector within the preceding 0.6 s; this coincidence implies an exceptionally low probability for the measured decay chains having a random origin (see Supplementary Information section 3). Instead, the observations are consistent with the decay properties of $^{283}\text{112}$ and ^{279}Ds inferred¹² from the experiments with the Dubna gas-filled recoil separator (Fig. 2). The current experiment did not confirm the initial observation of $^{283}\text{112}$ and its decay purely by spontaneous fission with a half-life of about 3 min^{14,15}.

The primary fusion product $^{287}\text{114}$ has a half-life of about 0.5 s, making it too short-lived to be transported to the COLD detector and thus allowing only the decay of the daughter nuclei $^{283}\text{112}$ and ^{279}Ds to be detected. Still, this observation represents a first independent confirmation of the production of element 112 and Ds in the nuclear fusion reaction of ^{48}Ca with ^{242}Pu . Furthermore, the independent confirmation of the decay properties of the isotope $^{283}\text{112}$ and its daughter ^{279}Ds substantiates the discovery in the more recent FLNR experiments¹² that $^{287}\text{114}$ and $^{291}\text{116}$ decay via alpha particle emission to $^{283}\text{112}$ and ^{279}Ds , respectively.

The observation that the two atoms of element 112 were transported through the experimental set-up to their deposition positions is indicative of a high volatility of this element (see also Supplementary Information section 1). In the first part of the experiment the inlet of the detector array was held at -24°C , allowing the cold end of the detector to reach its minimum temperature of -184°C and thus ensuring efficient deposition of the major part of radon-like species in the detector. Figure 3a gives the distribution of ^{185}Hg , ^{219}Rn and $^{283}\text{112}$ deposited in the detector array. About

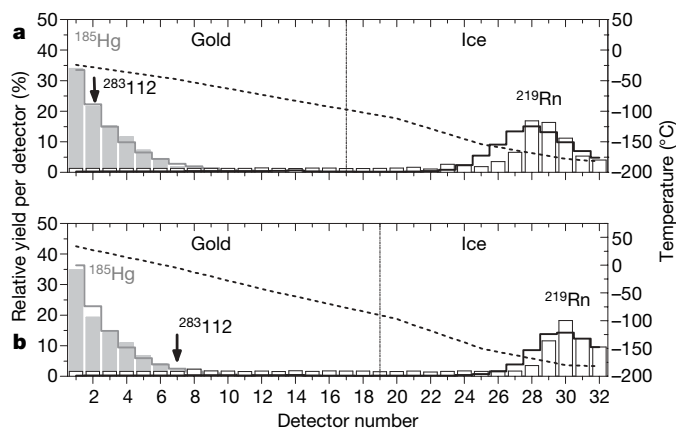


Figure 3 | Results of thermochromatographic separations of element 112 compared to mercury and radon in the COLD detector. The relative yields (left-handed axis) of ^{185}Hg (grey bars) and ^{219}Rn (white bars) are shown together with the two observed decays of $^{283}\text{112}$ (black arrows) as a function of the detector number. The results of a microscopic model of the adsorption process based on a Monte Carlo approach³⁰ are presented (solid lines). The vertical dashed-dotted lines indicate the beginning of the ice coverage of the gold surface at temperatures below -95°C . **a**, First part of the experiment: Monte Carlo simulations with adsorption enthalpies of $-\Delta H_{\text{ads}}^{\text{Au}}(\text{Hg}) > 47 \text{ kJ mol}^{-1}$ (grey solid line) and $-\Delta H_{\text{ads}}^{\text{Au}}(\text{Rn}) = 20 \text{ kJ mol}^{-1}$ (black solid line), are shown, respectively. The black dashed line (right-handed axis) represents the temperature gradient applied (-24 to -184°C). **b**, Second part of the experiment: Monte Carlo simulations with adsorption enthalpies of $-\Delta H_{\text{ads}}^{\text{Au}}(\text{Hg}) > 65 \text{ kJ mol}^{-1}$ (grey solid line) and $-\Delta H_{\text{ads}}^{\text{Au}}(\text{Rn}) = 20 \text{ kJ mol}^{-1}$ (black solid line) are shown, respectively. The black dashed line (right-handed axis) represents the temperature gradient applied ($+35$ to -180°C).

88% of the ^{219}Rn produced in the experiment was deposited on the last eight detectors, while the other 12% decayed in-flight when passing through detectors 1 to 24 (that is, about 0.5% decayed per detector pair). Deposition of ^{185}Hg on the gold surface occurred in the first detectors, that is, between -24°C and -50°C (Fig. 3a). This pattern is indicative of spontaneous deposition controlled only by the diffusion of ^{185}Hg out of the carrier gas to the gold surfaces. Under these conditions the first atom of $^{283}\text{112}$ was detected on the second detector at a temperature of -28°C (Fig. 3a, black arrow).

The observed deposition pattern in COLD is reproduced in kinetic Monte Carlo simulations of the gas-adsorption chromatography experiment³⁰, making it possible to infer the adsorption enthalpies ($-\Delta H_{\text{ads}}^{\text{Au}}$) for the elements on gold (see also Supplementary Information, section 1). In the case of mercury, the observed deposition pattern on the gold surface gives a lower limit of $-\Delta H_{\text{ads}}^{\text{Au}}(\text{Hg}) > 47 \text{ kJ mol}^{-1}$, while successful transport of the element at room temperature (20°C) through 8 m perfluoroalkoxy-Teflon capillary, in conjunction with empirical correlations, provides an upper limit of $-\Delta H_{\text{ads}}^{\text{Au}}(\text{Hg}) < 125 \text{ kJ mol}^{-1}$ (see Supplementary Information, section 1). Both limits are in agreement with literature data of $-\Delta H_{\text{ads}}^{\text{Au}}(\text{Hg}) = 98 \pm 3 \text{ kJ mol}^{-1}$ (ref. 29.). The deposition pattern of radon translates into an adsorption enthalpy of $-\Delta H_{\text{ads}}^{\text{Au}}(\text{Rn}) = 20 \pm 1 \text{ kJ mol}^{-1}$, which is somewhat lower than the literature value²⁷ of $-\Delta H_{\text{ads}}^{\text{Au}}(\text{Rn}) = 29 \pm 3 \text{ kJ mol}^{-1}$ for radon adsorption on gold surfaces. But it agrees well with the measured value of $-\Delta H_{\text{ads}}^{\text{ice}}(\text{Rn}) = 20 \pm 2 \text{ kJ mol}^{-1}$ for radon adsorption on ice surfaces³¹. This agreement and the observation that the dew point in the carrier gas was colder than -95°C points to a water content of < 0.1 p.p.m., suggesting that a thin ice layer covers the surfaces of the detectors that are kept at temperatures below -95°C . The observation in the first part of the experiment of element 112 in the main deposition region of mercury suggests a high probability for this atom having been deposited upon first contact with the gold surface.

The second part of the experiment was performed after raising the temperature at the inlet of the detector array to 35°C , the maximum temperature allowing safe operation of the silicon detectors. The increased inlet temperature leads to a temperature of -180°C at the cold end of the thermochromatography channel (Fig. 3b). Under these conditions about 65% of the ^{219}Rn deposited on the last five detectors, which according to the kinetic Monte Carlo model corresponds to a value of $-\Delta H_{\text{ads}}^{\text{ice}}(\text{Rn}) = 20 \pm 1 \text{ kJ mol}^{-1}$ that is consistent with the first measurement. For mercury, the diffusion-controlled deposition pattern of ^{185}Hg on the gold surface within the first eight detectors corresponds to a lower limit of $-\Delta H_{\text{ads}}^{\text{Au}}(\text{Hg}) > 65 \text{ kJ mol}^{-1}$, again consistent with the known adsorption data for mercury on gold²⁹. The second atom of $^{283}\text{112}$ to be observed in this study deposited on the seventh detector, held at -5°C . We note that only about 5% of the entire mercury reached this detector or deposited at lower temperatures (Fig. 3b).

The alpha particle decay of the $^{283}\text{112}$ atoms was detected both times on the non-gold-covered side of the detector pairs, which then also detected the subsequent spontaneous fission decay attributed to ^{279}Ds . This suggests that the alpha-decay daughter ^{279}Ds was recoil-implanted into the gold-covered detector owing to the momentum transfer during the alpha particle emission from $^{283}\text{112}$; otherwise, the recoiling ^{279}Ds would have been stopped in the carrier gas between the detectors and transported downstream to another detector pair. Therefore, we conclude that $^{283}\text{112}$ was deposited on the gold-covered side of the detector (see also Supplementary Information section 1).

The statistical Monte Carlo approach to modelling the gas chromatography results^{17,30} uses adsorption enthalpy values to mimic the observed deposition patterns, which provides upper and lower limits for the adsorption enthalpy of element 112 on gold $-\Delta H_{\text{ads}}^{\text{Au}}(\text{E112})$ of 98 kJ mol^{-1} and 45 kJ mol^{-1} (68% confidence interval), respectively; it also yields a most probable value of $-\Delta H_{\text{ads}}^{\text{Au}}(\text{E112}) = 52 \text{ kJ mol}^{-1}$, which has a large associated uncertainty due to the

small number of observed events (see also Supplementary Information section 2). Still, the range of likely adsorption enthalpies inferred from this study indicates an interaction between element 112 and gold that is significantly stronger than the purely dispersive van der Waals interactions of noble-gas like elements²⁷. We therefore conclude that the stronger adsorption interaction of element 112 with gold involves formation of a metal bond, which is behaviour typical of group 12 elements.

Received 27 July 2006; accepted 19 March 2007.

- Schädel, M. *et al.* Chemical properties of element 106 (seaborgium). *Nature* **388**, 55–57 (1997).
- Eichler, R. *et al.* Chemical characterization of bohrium (element 107). *Nature* **407**, 63–65 (2000).
- Düllmann, Ch. E. *et al.* Chemical investigation of hassium (Hs, element 108). *Nature* **418**, 859–862 (2002).
- Fricke, B. Superheavy elements. *Structure Bonding* **21**, 90–144 (1975).
- Pyykkö, P. & Desclaux, J.-P. Relativity and the periodic system of elements. *Acc. Chem. Res.* **12**, 276–281 (1979).
- Schwerdtfeger, P. & Seth, M. in *Encyclopaedia of Computational Chemistry* Vol. 4 2480–2499 (Wiley, New York, 1998).
- Yakushev, A. B. *et al.* First attempt to chemically identify element 112. *Radiochim. Acta* **89**, 743–745 (2001).
- Yakushev, A. B. *et al.* Chemical identification and properties of element 112. *Radiochim. Acta* **91**, 433–440 (2003).
- Gäggeler, H. W. *et al.* Chemical and nuclear studies of hassium and element 112. *Nucl. Phys. A* **734**, 208–212 (2004).
- Gregorich, K. E. *et al.* Attempt to confirm superheavy element production in the ⁴⁸Ca + ²³⁸U reaction. *Phys. Rev. C* **72**, 014605 (2005).
- Eichler, R. *et al.* Attempts to chemically investigate element 112. *Radiochim. Acta* **94**, 181–191 (2006).
- Oganessian, Yu. Ts. *et al.* Measurements of cross sections and decay properties of the isotopes of elements 112, 114, and 116 produced in the fusion reactions ^{233,238}U, ²⁴²Pu, and ²⁴⁸Cm + ⁴⁸Ca. *Phys. Rev. C* **70**, 064609 (2004).
- Hofmann, S. *et al.* The new element 112. *Z. Phys. A* **354**, 229–230 (1996).
- Oganessian, Yu. Ts. *et al.* Synthesis of nuclei of the superheavy element 114 in reactions induced by ⁴⁸Ca. *Nature* **400**, 242–245 (1999).
- Oganessian, Yu. Ts. *et al.* Second experiment at VASSILISSA separator on the synthesis of the element 112. *Eur. Phys. J. A* **19**, 3–6 (2004).
- Eichler, B. Volatility properties of transactinides around Z=114 (prediction). *Kernenergie* [in German] **19**, 307–311 (1976).
- Pitzer, K. S. Are elements 112, 114, and 118 relatively inert gases? *J. Chem. Phys.* **63**, 1032–1333 (1975).
- Gaston, N., Opahle, I., Gäggeler, H. W. & Schwerdtfeger, P. Is eka-mercury (element 112) a group 12 metal? *Angew. Chem. Int. Edn* **46** (14) 2444–2447 (2007).
- Eichler, B. & Rossbach, H. Adsorption of volatile metals on metal surfaces and its application in nuclear chemistry. I. Calculation of adsorption enthalpies for hypothetical superheavy elements with Z around 114. *Radiochim. Acta* **33**, 121–125 (1983).
- Eliav, E., Kaldor, U. & Ishikawa, Y. Transition energies of mercury and ekamercury (element 112) by the relativistic coupled-cluster method. *Phys. Rev. A* **52**, 2765–2769 (1995).
- Seth, M., Schwerdtfeger, P. & Dolg, M. The chemistry of the superheavy elements. I Pseudopotentials for 111 and 112 and relativistic coupled clusters calculations for (112)H⁺, (112)F₂, and (112)F₄. *J. Chem. Phys.* **106**, 3623–3632 (1997).
- Pershina, V., Bastug, T., Jacob, T., Fricke, B. & Varga, S. Intermetallic compounds of the heaviest elements: the electronic structure and bonding of dimers of element 112 and its homolog Hg. *Chem. Phys. Lett.* **365**, 176–183 (2002).
- Sarpe-Tudoran, C. *et al.* Adsorption of super-heavy elements on metal surfaces. *Eur. Phys. J. D* **24**, 65–67 (2003).
- Pershina, V. & Bastug, T. Relativistic effects on experimentally studied gas-phase properties of the heaviest elements. *Chem. Phys.* **311**, 139–150 (2005).
- Eichler, B. *Metal Chemistry of Transactinides*. PSI Report 00–09, ISSN 1019–0643 (Villigen, 2000).
- Eichler, B. *Volatilization Properties of Transactinides from Metal Surfaces and Melts (Thermochemical Calculation)*. PSI Report 03–01, ISSN 1019–0643 (Villigen, 2002).
- Eichler, R. & Schädel, M. Adsorption of radon on metal surfaces: a model study for chemical investigations of elements 112 and 114. *J. Phys. Chem. B* **106**, 5413–5420 (2002).
- Düllmann, Ch. E. *et al.* IVO, a device for in situ volatilization and on-line detection of products from heavy ion reactions. *Nucl. Instrum. Meth. A* **479**, 631–639 (2002).
- Soverna, S. *et al.* Thermochemical studies of mercury and radon on transition metal surfaces. *Radiochim. Acta* **93**, 1–8 (2005).
- Zvara, I. Simulation of thermochemical processes by the Monte Carlo method. *Radiochim. Acta* **38**, 95–101 (1985).
- Eichler, B., Zimmermann, P. & Gäggeler, H. W. Adsorption of radon on ice surfaces. *J. Phys. Chem. A* **104**, 3126–3131 (2000).

Supplementary Information is linked to the online version of the paper at www.nature.com/nature.

Acknowledgements We are indebted to the staff of the U-400 cyclotron for providing intense beams of ⁴⁸Ca. This work was supported in part by the Russian Foundation for Basic Research and by the Swiss National Science Foundation.

Author Information Reprints and permissions information is available at www.nature.com/reprints. The authors declare no competing financial interests. Correspondence and requests for materials should be addressed to R.E. (robert.eichler@psi.ch).